



ELSEVIER

Surface Science 349 (1996) 97–110

  
surface science

# The adsorption and decomposition of formic acid on Cu{110}

M. Bowker <sup>\*</sup>, E. Rowbotham, F.M. Leibsle, S. Haq

*Department of Chemistry, University of Reading, Whiteknights, P.O. Box 224, Reading RG6 6AD, UK  
and IRC in Surface Science, Liverpool University, Liverpool L69 3BX, UK*

Received 31 May 1995; accepted for publication 7 November 1995

## Abstract

The reactive adsorption of formic acid (HCOOH) on oxygen dosed Cu(110) has been studied using a molecular beam system, TPD, LEED and STM. At low temperature the reaction is strongly oxygen coverage dependent. All coverages result in high reaction probability (0.8 at room temperature) for formic acid and, for less than 0.25 monolayers of oxygen there is complete oxygen clean-off, leaving formate on the surface in a  $c(2 \times 2)$  structure. At higher coverages the situation is more complex, with some oxygen remaining coadsorbed with the formate. The two adsorbates are then mainly phase separated into islands of  $c(6 \times 2)$  oxygen and  $(3 \times 1)$  formate. The two phases mutually compress each other due to pressure at the phase boundaries. The reaction stoichiometry is 2:1 formic acid:oxygen atoms in this temperature range. At higher temperatures ( $> 450$  K) the formate itself is unstable and decomposes during adsorption which results in a change of stoichiometry of the reaction; one molecule of formic acid removes an oxygen atom as water, and hydrogen evolution ceases. There is a range of temperature between 350 and 420 K for which the reaction becomes very difficult, and the reaction probability drops to  $\sim 0.1$ . It is proposed that this is due to rapid compression of much of the oxygen adlayer into the unreactive  $c(6 \times 2)$  structure by small amounts of formate. The reaction proceeds through a highly mobile, weakly held, “precursor” state on the surface, which is able to seek out the active sites on the surface, which are low in coverage at high levels of oxygen. These active sites are the terminal oxygen atoms in the oxygen islands (in the [001] direction), which are only present at step edges or phase boundaries at 0.5 monolayers coverage of oxygen.

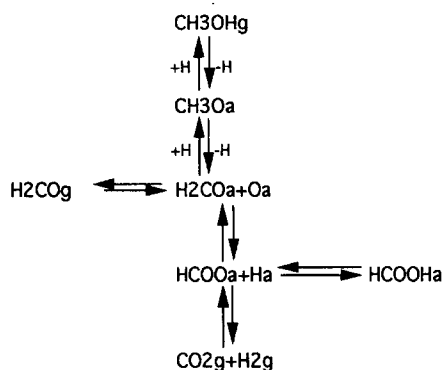
**Keywords:** Adsorption kinetics; Alcohols; Catalysis; Copper; Cu(110); Molecule-solid reactions; Oxygen; Scanning tunneling microscopy; Sticking

## 1. Introduction

The adsorption of formic acid on Cu is of both fundamental and practical interest. It is of fundamental interest because it represents the simplest carboxylic acid and it tends to form strong, bidentate intermediates on surfaces, being very stable on Cu in

particular. Madix was the first to study this adsorption system in any detail, using TPD [1–3], photoelectron spectroscopies [3] and synchrotron radiation (NEXAFS) [4]. Since then other work has been carried out using IRAS [5,6] and surface EXAFS has identified its orientation [7]. The formate appears to orient its molecular plane in the [011] azimuth and is essentially upright on the surface [7] with its two oxygens bound in equivalent environments [3,7]. The formate is stable up to 450 K when it decomposes by

<sup>\*</sup> Corresponding author.



Scheme 1. Methanol synthesis and decomposition.

C–H bond cleavage to yield  $\text{CO}_2$  and  $\text{H}_2$  in the gas phase with first order kinetics [1–3].

A study of formic acid adsorption is of practical interest because a number of studies have shown that the formate intermediate is directly involved in methanol synthesis from syngas (in this case a mixture of  $\text{CO}$ ,  $\text{CO}_2$  and  $\text{H}_2$ ). This is true for the original  $\text{ZnO}$  based catalysts [8] and for the lower pressure  $\text{Cu}$  based catalysts [9,10]. It has been shown that formate species can be formed from  $\text{CO}_2$  and  $\text{H}_2$  [11] and that, in turn, this can be hydrogenated to methanol [8–10]. It has been proposed that formate hydrogenation may be the rate determining step in

methanol synthesis ([10], and references therein), though this is not yet conclusively proven. A simplified mechanistic scheme, then, for methanol production can be written as shown (Scheme 1). This shows the pivotal role of the formate in the process.

Clearly, then, it is important to understand the detailed kinetic and structural factors involved in all these steps, and this is a focus of the ongoing work in our laboratory which is concentrating on the adsorption of  $\text{CH}_3\text{OH}$ ,  $\text{H}_2\text{CO}$  and  $\text{HCOOH}$  in UHV conditions. In this work we report for the first time, detailed kinetic studies of formic acid adsorption and reaction on  $\text{Cu}\{110\}$  mainly using molecular beam reaction spectroscopy, but also combined with TPD and STM. In another publication we will report in more detail on structural studies of this adsorption system using LEED and STM. All these measurements were carried out on both clean and oxygen precovered  $\text{Cu}\{110\}$ .

## 2. Experimental

The work was carried out in a UHV machine constructed by VSW LTD (Manchester, UK) which is shown in Fig. 1. It consists of a combined thermal molecular beam/FTRAIRS facility, and also com-

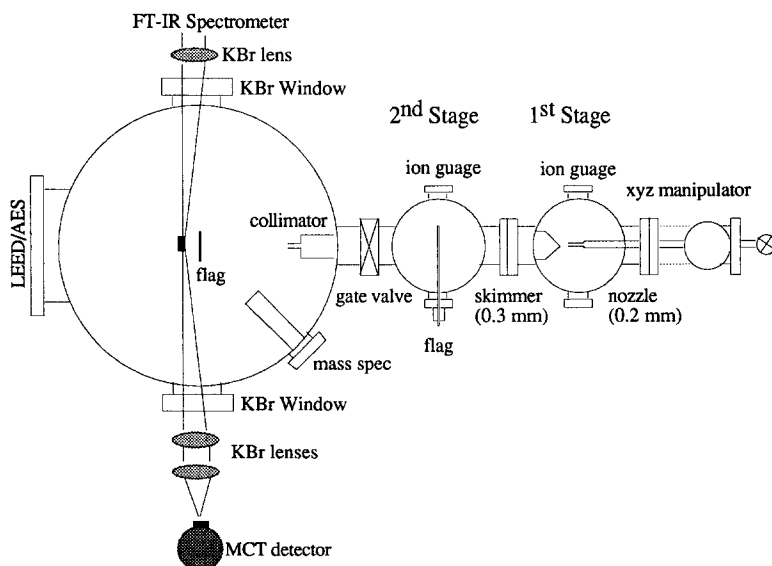


Fig. 1. Plan schematic of the instrument used in this work for LEED, molecular beam and TPD studies.

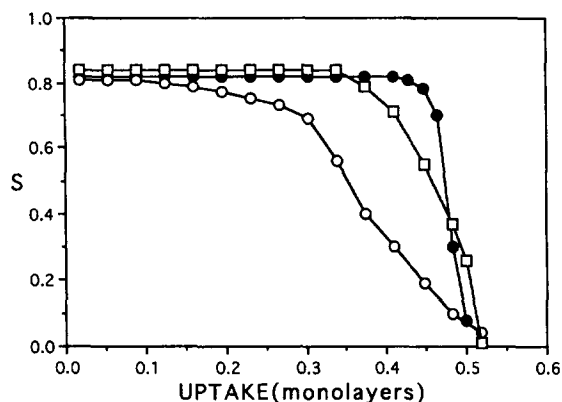


Fig. 2. Comparison of the sticking probability for formic acid adsorption on Cu(110) at 300 K, with different precoverages of atomic oxygen. (●) are for 0.25 monolayers of oxygen preadsorbed, (○) for 0.5 monolayers, while (□) are for adsorption on the 0.5 monolayer predosed surface after dosing with formic acid (that is adsorption as for the previous curve), then TPD to remove the formate and cooling. The latter curve is similar to that for the 0.25 monolayer case.

prises a rear view LEED/Auger system (VG Scientific). The thermal molecular beam is basically of the same design as that described earlier [12], except that the beam size at the sample is bigger at 7 mm diameter. The preparation of the crystal and gases was carried out in the standard manner described previously [12].

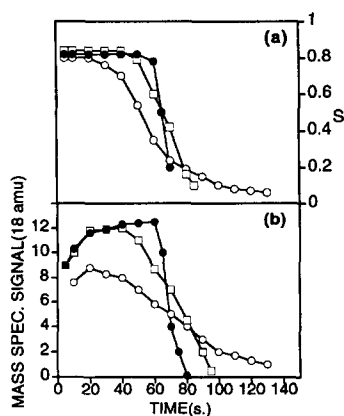


Fig. 3. (a) The dependence of formic acid sticking probability on time, for the same experiments shown in Fig. 2. (b) Water evolution (the only product at this temperature) for the adsorption measurements of (a).

### 3. Results

#### 3.1. Molecular beam reaction spectroscopy

##### 3.1.1. Clean surface

The sticking probability of formic acid on the clean Cu(110) surface is low in the temperature range of measurement (above 300 K) and was not investigated in any detail since the accuracy of our measurement ( $\pm 0.02$  on an individual run) resulted in poor accuracy of the coverage dependence of sticking. The value of the initial sticking coefficient at 300 K is  $0.1 (\pm 0.02)$ .

##### 3.1.2. Oxygen predosed surface

Oxygen was predosed onto the surface from the molecular beam source. The initial sticking coefficient (0.21 at 300 K) and its coverage dependence

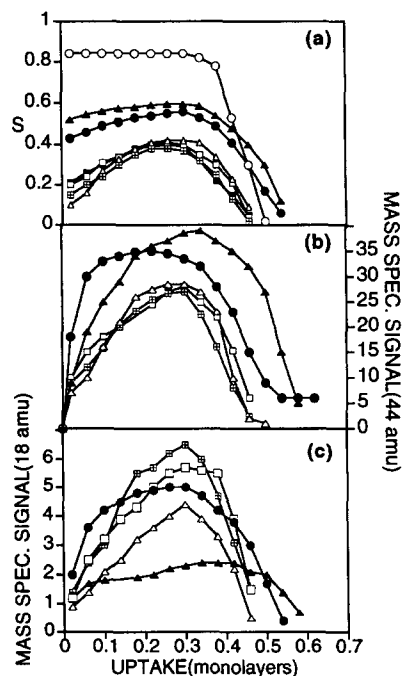
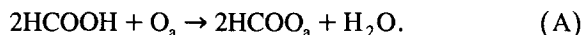


Fig. 4. (a) Coverage and temperature dependence of the sticking probability for formic acid adsorption on the Cu(110) surface predosed with 0.5 monolayers of oxygen atoms. The adsorption temperatures are as follows: (○) 343 K, (▲) 448 K, (●) 473 K, (■) 523 K, (□) 573 K, (⊞) 673 K, (△) 773 K. (b) Carbon dioxide evolution during formic acid adsorption, corresponding with the curves in (a). The evolution rate is immeasurably slow below 400 K. (c) Water evolution during formic acid adsorption, corresponding with the curves in (a).

was measured to be similar to that described in detail previously [13], and in this way we could accurately predose the surface with gas.

Fig. 2 shows the results for the sticking probability of formic acid on the surface as a function of uptake. For 0.25 monolayer of predosed oxygen (defined with respect to the clean surface number density of Cu atoms in the top layer) the initial sticking coefficient was high at  $0.82 (\pm 0.01)$  where the number in the brackets denotes the mean deviation of the data (that is, several runs). Water is coincidentally desorbed from the surface during the

adsorption process, as shown in Fig. 3 and discussed below, due to formate formation with the following overall reaction stoichiometry:



It is very noticeable that as the uptake of formic acid increases, nevertheless the sticking probability remains constant to very high coverage ( $\sim 0.4$  ML). This indicates the involvement of a weakly held precursor state to dissociation in the adsorption kinetics [14–16] and this is discussed in more detail below. The uptake saturates at  $0.5 (\pm 0.03)$  mono-

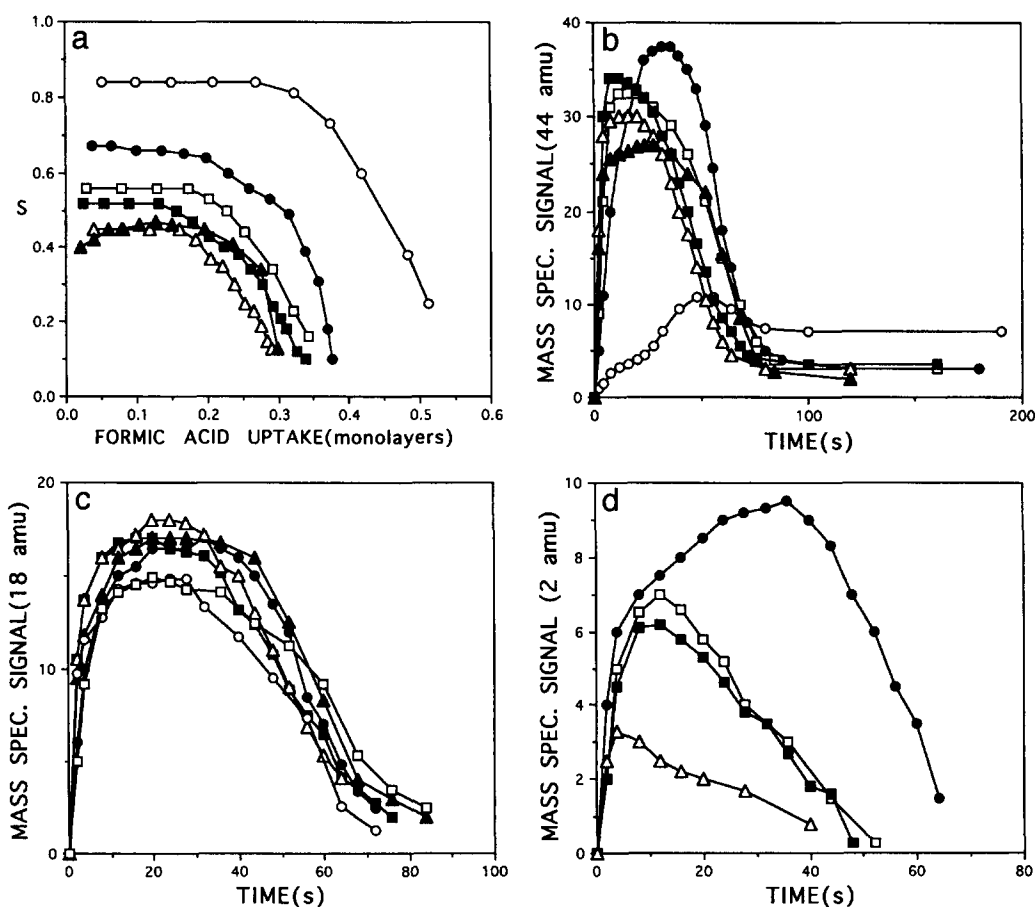


Fig. 5. (a) Coverage and temperature dependence of the sticking probability for formic acid adsorption on the Cu(110) surface predosed with 0.25 monolayers of oxygen atoms. The adsorption temperatures are as follows: (○) 420 K, (●) 448 K, (□) 473 K, (■) 523 K, (△) 573 K, (▲) 673 K. (b) Carbon dioxide evolution during formic acid sticking, corresponding with the curves in (a). (c) Water evolution during formic acid sticking, corresponding with the curves in (a). (d) Hydrogen evolution curves during formic acid adsorption corresponding with those in (a). The evolution below 440 K is at a very low rate and is not shown due to limited accuracy; above 600 K there is no hydrogen evolution within the accuracy of our measurements.

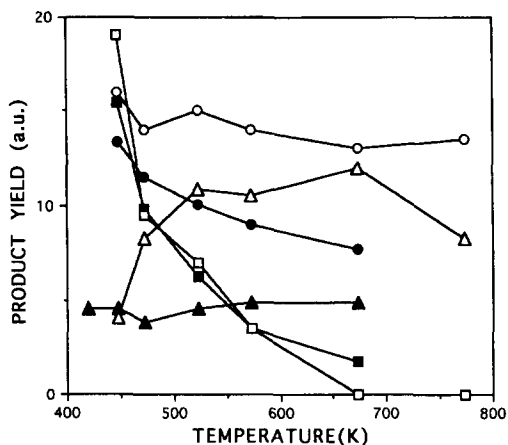


Fig. 6. Adsorption temperature dependence of the product yield for formic acid adsorption on 0.25 and 0.5 monolayers of preadsorbed oxygen atoms. Half monolayer predose; (○) carbon dioxide, (△) water, (□) hydrogen; quarter monolayer predose; (●) carbon dioxide, (▲) water, (■) hydrogen.

layers for this oxygen predose. If the 1/4 monolayer of oxygen was annealed to 520 K before cooling to 300 K and subsequently carrying out the formic acid sticking measurements, the only difference was that the sticking coefficient stayed at 0.82 up to a coverage of  $\sim 0.45$  monolayers. After such an experiment, the surface was heated to 550 K to decompose the adsorbed formate (producing  $\text{CO}_2$  and  $\text{H}_2$ , Section 3.2 below), then the surface was clean and free of oxygen as endorsed by the lack of water evolution on subsequent exposure to formic acid, and the low value of the sticking coefficient ( $\sim 0.1$ ).

When 1/2 monolayer of oxygen atoms were first adsorbed on the surface then the curve was a little different as shown in Fig. 2. The initial sticking coefficient was the same but the dependence upon coverage is more curved with the  $S$  value decreasing after an uptake of only 0.2 monolayers. The total formic acid uptake is then the same as for 1/4 monolayer of oxygen predosed. If, however, the adsorbed layer was heated to 550 K to decompose the formate, the sample was cooled and then formic acid was reintroduced, the sticking coefficient was characteristic of a surface with oxygen present and the curves look similar to those for 1/4 monolayer of oxygen predosed. These measurements show that about 0.25 monolayers of oxygen were left on the

surface after the first reaction with formic acid, that is, only half was reacted away.

Fig. 3 shows the dependence of sticking probability upon time for the same experiments as in Fig. 2 and shows also that the evolution of water (the only product at these adsorption temperatures) is coincident with the adsorption, that is, water formation is not slow or rate limiting. The amount of water evolved is the same whether 1/4 or 1/2 monolayer of oxygen was predosed, and is similar for a second dose of formic acid onto a surface which had been previously dosed with 1/2 ML oxygen, reacted with formic acid and then decomposed by heating, confirming the finding that only half of the oxygen adlayer reacts at room temperature.

### 3.1.3. Temperature effects

Figs. 4 and 5 show a series of experimental results at different temperatures for formic acid reacting with 0.5 and 0.25 monolayers of predosed oxygen respectively. For the 1/2 monolayer oxygen the only product below 400 K is water due to the stability of the formate species on the surface. Above this temperature however, the formate is unstable on the surface and so decomposes to yield products of  $\text{CO}_2$  and  $\text{H}_2$  from the surface. As the temperature increases so the hydrogen product ceases to evolve and the lineshape of the  $\text{CO}_2$ ,  $\text{H}_2\text{O}$  and formic acid uptake curves change. The initial sticking coefficient is now lower, but rises during adsorption and the

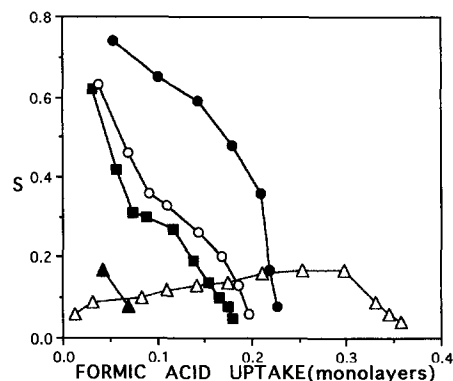


Fig. 7. Sticking probability dependence on uptake in the temperature range of unusually low reactivity with 0.5 monolayers of preadsorbed oxygen: (●) 353 K, (○) 373 K, (■) 383 K, (▲) 403 K and (△) 413 K.

CO<sub>2</sub> evolution rate increases to a maximum before dropping again as the predosed oxygen is all used up. Note however that the CO<sub>2</sub> evolution does not return to zero above about 450 K, but has a definite rate due to formate decomposition on the clean surface. The measurements show both a decreasing initial rate of CO<sub>2</sub> evolution/HCOOH adsorption and a decreasing steady state CO<sub>2</sub> evolution from the clean surface as substrate temperature increases. The

clean surface rate of decomposition is evident at long times after the transient oxygen clean-off reaction has finished (Fig. 5b).

The curves for the 0.25 monolayer dose (Fig. 5) are a little different. The initial sticking coefficients are less temperature sensitive (and appear to be close to the values for the half monolayer case when half the reactive oxygen has been removed), and show a marked decrease in the saturation uptake as tempera-

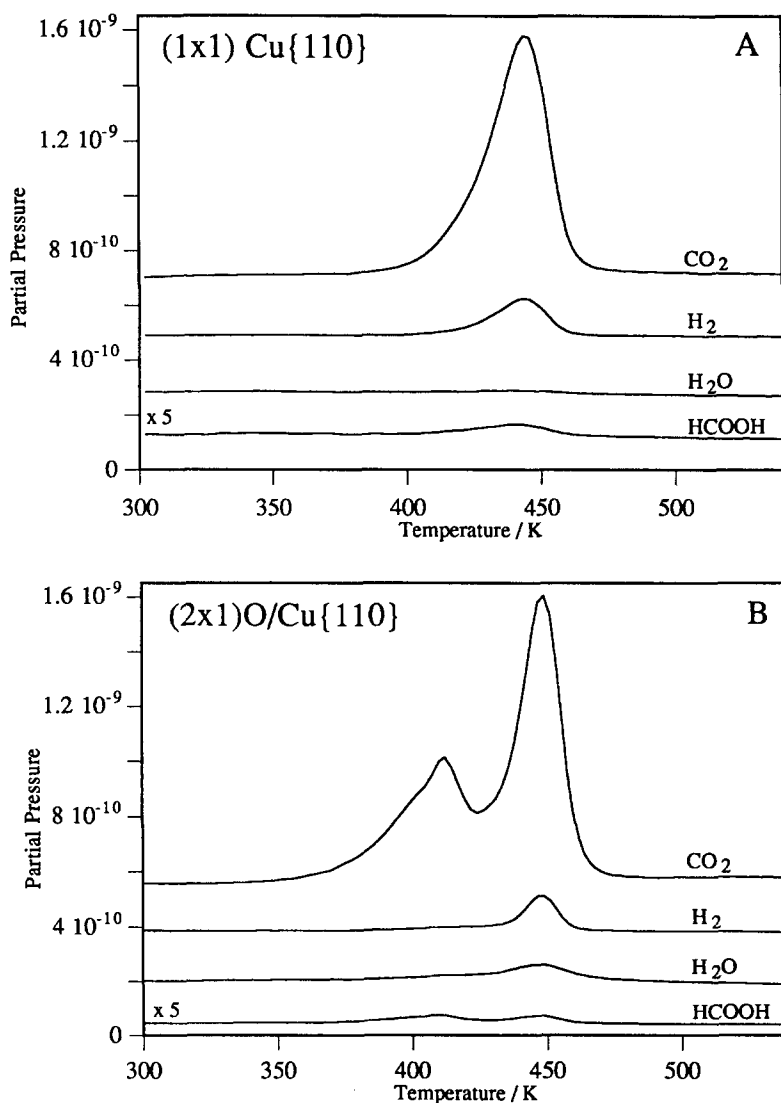
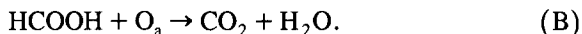


Fig. 8. TPD spectra for formic acid decomposition on (A) the clean Cu(110) surface at saturation coverage and from (B) the surface predosed with 0.5 monolayers of oxygen, both dosed onto the crystal at 300 K.

ture increases. The uptake decreases from 0.5 monolayer to 0.25, that is, a decrease in the reaction ratio of formic acid to atomic oxygen from 2:1 to close to 1:1. This is a similar effect to that found previously for the reaction of methanol with this surface [18]. There is not such an apparent initial region of low product evolution rate (Figs. 5b–d) as there was for the 0.5 monolayer case (Figs. 4b and 4c), except at the low temperature of 420 K where the formate stability is relatively high. This is due to the high initial sticking coefficient in this case.

The integrated yields of products are shown as a function of temperature in Fig. 6, for both oxygen coverages and show the reduction in hydrogen evolution above 400 K. The water evolution is constant, within experimental uncertainty, for the 0.25 monolayer oxygen case. For the 0.5 monolayer oxygen surface, however, only half the surface oxygen is reacted below  $\sim 450$  K and so the same amount of

water is liberated as for the 0.25 monolayer oxygen case. At higher temperatures ( $> 500$  K) all the oxygen is removed, so the water yield is doubled. For  $\text{CO}_2$  production, increasing temperature reduces the yield by nearly a factor of two in the 0.25 monolayer  $\text{O}_a$  case, reflecting the change in overall stoichiometry from that shown above (reaction A, which results in two molecules of  $\text{CO}_2$  being evolved from formate decomposition) to the following.



The reason that the  $\text{CO}_2$  evolution remains essentially constant for the 0.5 monolayer oxygen predose over the temperature range is that, together with this stoichiometry change, there is also a doubling of the amount of oxygen used up as the temperature increases and the formate becomes unstable.

There is a region of unusual behaviour for this system between 340 and 410 K, but only for the case

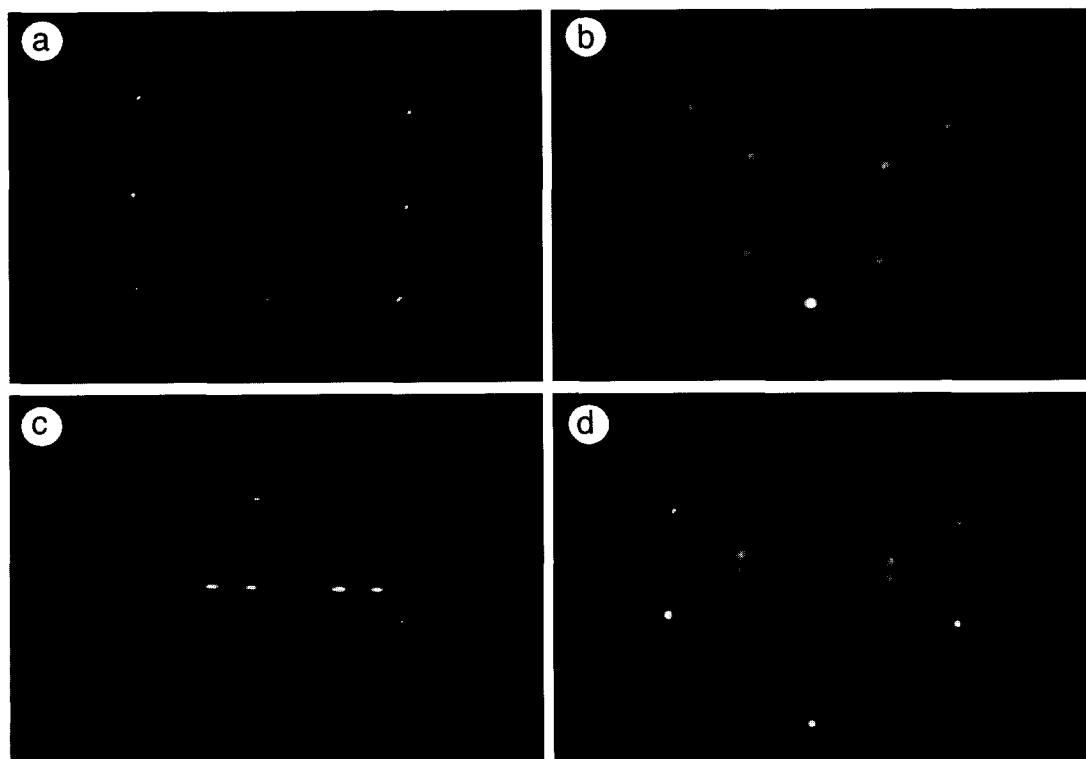


Fig. 9. Leed patterns from (a) the clean Cu(110) surface (at 77 V), (b) the  $c(2 \times 2)$  surface after dosing 3 L of formic acid onto 0.25 monolayers of atomic oxygen (at 80 V), (c) the surface after 3 L of formic acid onto 0.5 monolayers of atomic oxygen (56 V), showing a mixed  $c(6 \times 2)/p(3 \times 1)$  and (d) exhibiting the "split  $c(2 \times 2)$ " when  $\sim 0.3$  monolayers of atomic oxygen was predosed (66 V).

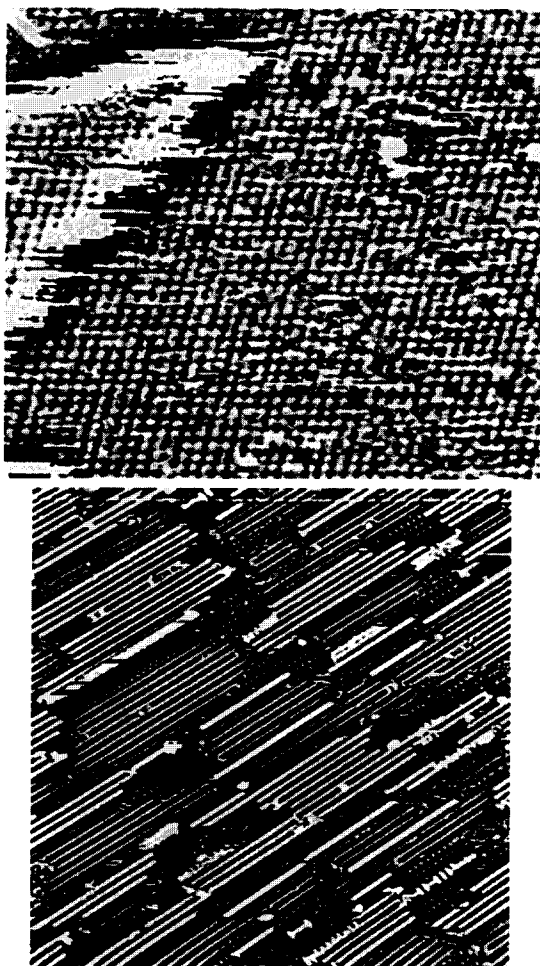


Fig. 10. STM images of the Cu(110) surface showing (a) the  $c(2 \times 2)$  structure after HCOOH reaction with 0.25 ML of pre-dosed oxygen (imaged area  $20 \text{ nm} \times 20 \text{ nm}$ ), and (b) the mixed structures ( $c(6 \times 2)/p(3 \times 1)$  and small areas of  $c(2 \times 2)$ ) formed after formic acid adsorption on 0.5 ML of oxygen (imaged area  $30 \text{ nm} \times 30 \text{ nm}$ ).

of 0.5 monolayers of predosed oxygen. Here the adsorption begins with high probability but then drops to low values without the extent of reaction seen at other temperatures; this is shown in Fig. 7. At the lower end of this temperature range the initial sticking coefficient is as it is at 300 K, but drops rather more quickly as the coverage increases. As the temperature increases in this range, so the initial sticking goes down, as also does the uptake, the most extreme example of this being at 403 K, where little adsorption at all is detected. At 413 K the character-

istics of the adsorption are changing to become more like those at more elevated temperatures, that is the adsorption probability is low to begin with and then slowly rises with time and reaction.  $\text{CO}_2$  is slowly evolved after the initial adsorption at this temperature. The cause of this very surprising behaviour is discussed in more detail below.

### 3.2. Temperature programmed desorption

Figs. 8a and 8b show TPD profiles from the clean Cu{110} surface and that dosed with oxygen. These data look similar to those reported earlier by Bowker and Madix [3]; in particular, the spectra show a shoulder at the leading edge ( $\sim 430 \text{ K}$ ) for the  $1/2$  monolayer O predosed surface, after a saturation coverage of the formate species is adsorbed. The desorption from the clean surface and that with  $1/4$  ML oxygen predosed shows classical first order desorption kinetics, that is, with a peak shape asymmetric with respect to the peak temperature, and with a peak temperature which is independent of coverage.

It must be noted there is evidence of small amounts of molecular formic acid desorption coincident with the formate decomposition, as reported earlier by Bowker and Madix [3] and since by others [17]. Secondly, only a small amount of water is produced, even though oxygen is coadsorbed with the formate for the 0.5 monolayer oxygen predose. If, after the TPD experiment shown in Fig. 8b, the sample is cooled and formic acid readsorbed at room temperature, subsequent TPD is similar to that in spectrum A.

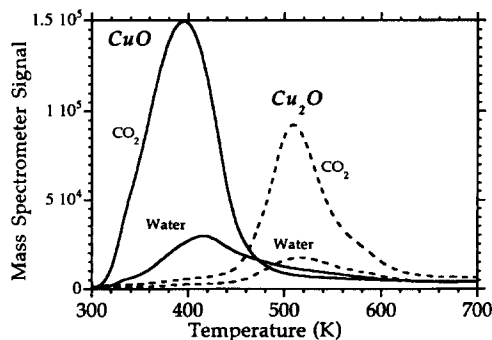


Fig. 11. Comparative TPD spectra after formic acid adsorption on powdered samples of Cu(I) and (II) oxides, showing the very different stability of the species on these surfaces [21].



### 3.3. Surface structure

No ordered adsorbate LEED patterns were seen for the adsorption of formic acid on the clean Cu(110) surface, even though formate was present as evidence by subsequent TPD. With 1/4 ML of oxygen preadsorbed, subsequent acid adsorption at 300 K results in a sharp well ordered  $c(2 \times 2)$  pattern (see Fig. 9b). With 1/2 ML of preadsorbed oxygen the resulting pattern is more complex, but appears to be a coexistence of  $p(3 \times 1)$  and  $c(6 \times 2)$  as shown in Fig. 9c. With an oxygen predose of more than 1/4 ML the sequence is more complex still with the  $(1/2, 1/2)$  spots split (Fig. 9d). If this layer is warmed to 400 K, the splitting is eliminated and a very sharp  $c(2 \times 2)$  is again obtained. All these LEED images are reasonably stable with time in the electron beam, in complete contrast to another system we have recently studied [18,19] for which methoxy intermediates were unstable in the electron beam.

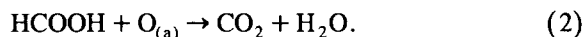
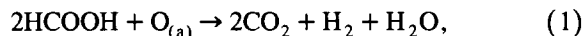
STM images of the  $c(2 \times 2)$  structure and the mixed layer are shown in Fig. 10. The  $c(2 \times 2)$  is particularly well ordered over the long range, hence the sharpness of the spots in the LEED. The mixed layer shows a very heterogeneous surface with small islands of  $c(6 \times 2)$  and  $p(3 \times 1)$  structures with a small amount of  $c(2 \times 2)$ . The dominant formate-induced structure for adsorption on the oxygen half monolayer at temperatures above  $\sim 350$  K is a  $p(4 \times 1)$ , which, in STM, appears to consist of alternate rows of oxygen and formate in the (001) direction. A detailed study of this adsorption system using STM will be reported elsewhere [20].

## 4. Discussion

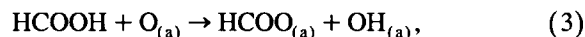
### 4.1. Mechanism

The mechanism and the overall stoichiometry of this reaction has already been reported from TPD studies as that below (reaction 1), but the advantage of the molecular beam is that it can be used study such reactions at high temperatures where the formate intermediate is unstable. TPD necessarily has to study layers adsorbed below the desorption temperature. As a result we have discovered that the mecha-

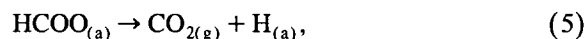
nism of this reaction changes with substrate temperature, as was also the case for the methanol oxidation reaction on this surface [18], with a change in overall stoichiometry from (1) to (2) below as the surface temperature increases.



This is evidenced by (a) the lack of  $\text{H}_2$  evolution at high temperature and (b) the reduction in  $\text{CO}_2$  evolution and  $\text{HCOOH}$  uptake for the 1/4 monolayer case (Fig. 5), while the  $\text{H}_2\text{O}$  evolution remains the same. The reason for this change in stoichiometry is the same as for the partial oxidation of methanol [18] and is simply due to the stability of the formate intermediate, which is high at 400 K, but low at 600 K (that is, on each side of the TPD peak). Thus for the low temperature regime the following steps take place.



Hence the 2:1 stoichiometry seen in previous TPD studies with 1/4 monolayer of oxygen preadsorbed. If such a layer is then heated the formate decomposes at  $\sim 440$  K to give  $\text{H}_2$  and  $\text{CO}_2$  in a 1:2 ratio [1–3], hence the overall reaction stoichiometry shown in Eq. (1) above. However, at more elevated adsorption temperatures the following steps occur after step 3.



Thus the OH formed is immediately mopped up by the hydrogen from formate decomposition which occurs on a fast timescale compared with adsorption. In between the two temperature extremes there is a shift from hydrogen atom recombination (step 6, resulting in the overall stoichiometry of (1)) to solely  $\text{H}_2\text{O}$  production (step 7 and overall stoichiometry of Eq. (2)), as the formate stability decreases (that is, the rate constant for decomposition increases). Since the formate is relatively stable at low temperature, up to  $\sim 450$  K, there is little hydrogen around to “mop up” OH groups formed in step (3) and so OH is

instead mopped up by the acid group of the incoming molecules (step 4). Once it becomes very unstable at  $> 600$  K, only step (3) occurs and as soon as OH is formed, it is stripped off by hydrogen atoms (step (7)) which dominates over (6). In between these temperature extremes there is a switch from (6) to (7). This implies a higher activation energy for step (7).

#### 4.2. Kinetics

The important mechanistic steps are written above and indicate a fairly simple reaction, which is partly why formic acid decomposition has been used as a benchmark in catalytic studies over the years. The decomposition of formic acid has been measured by the TPD technique and yields the results shown in Fig. 8, indicating the presence of formate on clean Cu as already reported by others [1–3,17]. This decomposition is a rare case of classical first order kinetics with a peak temperature which is near invariant with coverage, at least in the range up to  $\sim 0.3$  monolayers. Our estimate of the coverage of formate on the clean surface is  $\sim 0.3$  monolayers, in agreement with previous findings [3,17]. This is deduced by comparison with the higher uptake on, for instance, a surface with  $1/4$  monolayer of pre-dosed oxygen where the adatom is titrated off to give water and  $1/2$  monolayer of formate in the characteristic  $c(2 \times 2)$  structure. With higher oxygen doses still, there is little measurable increase in the formate coverage, but the desorption changes as shown in Fig. 8 and as reported elsewhere [3,17]. It results in a lower energy pathway to formate decomposition and the evidence indicates that this is due to the presence of oxygen atoms on the surface during formate decomposition. These lower temperature states only appear when  $> 0.25$  monolayers of oxygen is pre-dosed, and under such circumstances not all the oxygen is consumed during adsorption at 300 K. Since most of the formate still decomposes at the same temperature, it is likely that the lower stability formate is associated with the oxygen – perhaps at the edge of the  $c(6 \times 2)$  oxygen islands. It is interesting to compare these data with desorption from powdered copper oxides [21] and Fig. 11 shows TPD after formic acid adsorption on these materials carried out in a separate piece of equipment. Here

comparison is made between the stability of formate on Cu(I) and (II) oxides. The CuO material shows a much lower stability of the formate (by  $\sim 100$  K), leading us to conclude that the low temperature form of formate from Cu(110) is indeed associated with the oxygen on the surface, but also that the surface oxide is Cu(II)-like. Indeed, we believe it is possible that this lower temperature form of desorption may be due to a more weakly bound monodentate version of the formate. This possibility is being investigated with other techniques, especially IR and will be reported in the near future.

The molecular beam measurements give considerable extra insight into the kinetics of the whole reaction. In terms of adsorption, formic acid has a much higher sticking coefficient on oxidised Cu than has methanol. In both cases oxygen activates the reactivity of the surface, but the maximum reaction probability of methanol is around 0.15 [18] above 300 K, whereas for formic acid it is  $> 0.8$ . Furthermore, at 300 K methanol has a very low reactivity ( $< 0.02$ ) with the  $1/2$  monolayer oxygen structure, whereas formic acid still has a high reactivity. This is discussed in more detail below.

For formic acid the sticking probability shows a shape which is indicative of the effect of a precursor state [16] which has high diffusivity in a weakly held layer. This enables the moving molecule to diffuse over inactive areas of the surface and find the active sites which may be present in low concentration. This keeps  $S$  high until nearly all the oxygen has been reacted away (for  $< 1/4$  ML  $O_{(ad)}$ ), when the value drops to the low adsorptivity characteristic of the clean surface (estimated to have a sticking probability of  $\sim 0.1$ ). For more than  $1/4$  ML oxygen pre-dosed, the reactivity stops after the adsorption of around  $1/2$  monolayer of formate (Fig. 2). However, this formate must be more concentrated than for the  $c(2 \times 2)$  layer, since it appears to be located on only part of the surface, because the formate and oxygen islands are phase separated. The STM images shown above indicate that this occurs partly by compression of the remaining oxygen atoms into a high local coverage  $c(6 \times 2)$  structure. This oxygen structure is the one that is left after reaction is completed and must be relatively unreactive to formic acid. Indeed, we have recently begun to examine the reactivity of the  $c(6 \times 2)$  layer, formed by using high doses of

oxygen, and the sticking probability of formic acid is low ( $< 0.07$ ) on this surface. This gives an explanation for why the sticking coefficient begins to drop earlier in total uptake for the 0.5 monolayer predose; as reaction proceeds, so some of the oxygen is converted to  $c(6 \times 2)$  which is unreactive, so the total number of active sites diminishes. These sites become so diluted that even with the high diffusivity of formic acid molecules, they have a less than unity value of finding the active site, a value which further diminishes as adsorption and adlayer compression continues.

For the case of the surface with  $1/2$  ML predosed oxygen atoms, the behaviour at intermediate sample temperatures is quite unusual. Here, the reactivity is high up to about 340 K and above 430 K, with the high value of the sticking probability continuing high for a significant period of time. However, in between these two temperature regimes the  $S_0$  value is high, but drops quickly after a short period of reaction the most extreme case of this being for adsorption at 403 K, as shown in Fig. 7. At 373 K, the high value of 0.8 for  $S_0$  precipitately drops to a low value, and there is little further apparent uptake. These effects are not observed for a layer with  $1/4$  ML predosed oxygen atoms.

There are two possible explanations for this behaviour, which relate to the structures of the adsorbed layer on the surface.

(1) *Active site poisoning*. It is possible that there is only a limited number of active sites on the surface and that the formic acid can find them with high probability due to diffusion in the weakly held precursor state. It may be that in the temperature range described above these sites cannot be freed once the formate has adsorbed at them. However, this explanation seems unlikely, since it would be surprising for these sites to remain available at lower temperatures where the experiments show the reaction to proceed well, at least up to 0.5 monolayers uptake of formic acid.

(2) *Formate induced restructuring of the oxygen layer*. This is a more likely explanation, especially as we have some evidence to support it from the LEED and STM images. For the room temperature experiments it appears that the formate adsorbs into a particular phase on the surface, namely, the  $p(3 \times 1)$  which must contain a high coverage of formate, as

described below. The reason this is postulated is that (i) half of the original oxygen is left on the surface (that is,  $1/4$  ML total); (ii) half a monolayer of formate has adsorbed (twice the amount of oxygen removed during adsorption as water); (iii) as seems to be indicated by the images of Fig. 9, each occupies only a part of the surface, thus the remaining oxygen and the formate are phase separated. It is clear from the STM and the LEED that a  $c(6 \times 2)$  phase is present, and this is a structure which is reported for a high coverage of oxygen on Cu{110} [22]. This would explain why the surface is no longer reactive after  $1/4$  ML of oxygen is removed – the rest of the oxygen is compressed into the higher coverage  $c(6 \times 2)$  which is relatively unreactive as described above.

At intermediate temperatures small amounts of formate results in self-poisoning and it is postulated that this is due to easier compression of the oxygen layer, presumably by easier diffusivity of the oxygen and Cu atoms which are required to form the double added row  $c(6 \times 2)$ , proposed by various workers [22–25]. At low temperature, under our conditions, the diffusion is slower and more areas of the relatively reactive  $p(2 \times 1)$ -O remain while the adsorption takes place. A further difference may be in the formate phase which is formed. It appears that at the more elevated temperatures a  $p(4 \times 1)$  phase of formate becomes more dominant and this appears to consist of alternate rows of formate and oxygen, the rows being oriented in the [001] direction on the surface. In effect the area per formate produced may be higher which will result in a lower coverage of formate compressing the oxygen into the  $(6 \times 2)$ , but also appears to result in the formation of isolated strings of oxygen in the  $(4 \times 1)$  which are not so readily available for reaction.

Analysis of some of the images for the room temperature reaction indicates that the area occupied by the  $c(6 \times 2)$  is about 25% of the total area, leaving the formate induced  $(3 \times 1)$  occupying the remaining 75% of the area. If the  $c(6 \times 2)$  is a 0.67 monolayer structure, as proposed by several authors [22–25], then the amount of oxygen associated with it is  $1/6$  of a monolayer on the basis of the coverage being averaged over the whole surface. From the reaction measurements, half of the oxygen is removed in the reaction, leaving  $1/4$  monolayer. That

is, some oxygen may be left associated with the formate layer, but this only amounts to  $1/12$  of a monolayer averaged over the whole surface, or  $1/9$  of a monolayer local coverage if it is only associated with the formate part of the surface. A difficulty here is associating the  $c(6 \times 2)$  with 0.67 monolayers of oxygen. If there is more oxygen in this structure then there may be none associated with the formate ( $3 \times 1$ ) islands, if less, then the oxygen associated with the formate may be higher.

Although the absolute reactivity of formic acid is higher than that for methanol, the form of the kinetics is similar. The 0.25 monolayer surface reacts relatively easily and quickly with the organic molecule, whereas the 0.5 monolayer surface shows (i) a low initial rate (only shown at  $> 370$  K for

formic acid), (ii) an induction time to maximum reaction rate at low temperatures and (iii) a maximum in  $S$  which occurs more quickly at elevated temperatures. For the methanol case STM shows quite clearly that this was due to the limited availability of “active sites” for the initial oxidative dehydrogenation reaction (which produces methoxy intermediates) at high oxygen coverages [18–20]. The active site was shown to be the oxygen atoms at the end of the  $p(2 \times 1)$  oxygen islands which are present at less than saturation oxygen coverage. At 0.5 monolayers of predosed oxygen the only appropriate sites are those at steps or defects in the oxygen adlayer. The reaction rate increases with time (autocatalysis) due to the creation of new active sites as the reaction proceeds. This process was shown in our

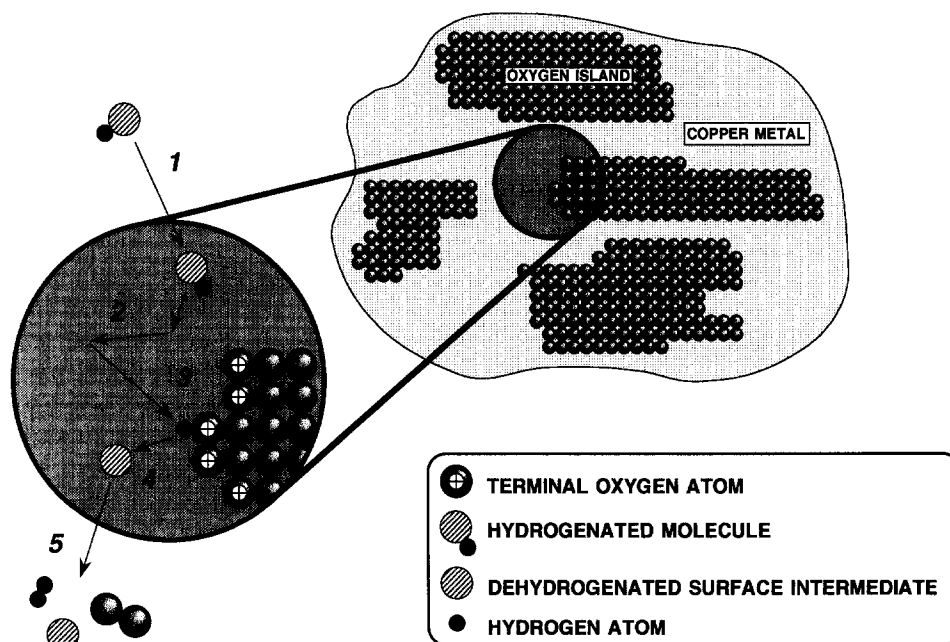
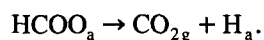
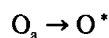
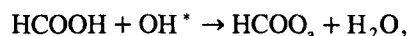
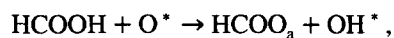


Fig. 12. A schematic model for the reaction of organic molecules (carboxylic acids and alcohols, for instance) with islands of oxygen on Cu(110). Here the islands are simplified to show only the oxygen atoms, whereas in reality they are an equiatomic mix of oxygen and copper atoms in a  $(2 \times 1)$  structure. The active sites for reaction are at the short ends of the islands where terminal (low coordination) oxygen atoms exist. The reaction occurs in several steps: (1) adsorption of the parent molecule; (2) diffusion in a weakly held state (probably physisorbed) over many surface sites (including those filled with oxygen); (3) impingement at an active site and reaction by attack of terminal oxygen at the reactive functional group of the molecule, resulting in deprotonation to form a hydroxyl group and a surface intermediate; (4) diffusion of the intermediate away from the active site and (5) decomposition of the intermediate to yield gas phase products. Note that the reaction can then proceed further by hydroxyl attack on another incoming molecule to form another intermediate and to produce water in the gas phase which, in turn, exposes a new active terminal oxygen species. In the specific case studied in this work the intermediate is the formate and the gas phase products are carbon dioxide, hydrogen and water.

earlier publication [18] to occur by the creation of holes in the oxygen adlayer at the steps which appear to diffuse relatively easily to the oxygen saturated terraces, creating terminal oxygen atoms in the islands of adsorbate. These reactions are illustrated in Fig. 12. In simple terms the mechanism can be written as follows:



The hydrogen produced in the latter reaction can then undergo either homonuclear recombination (step 6) or react with hydroxyl groups to produce water (step 7). The former is dominant at low temperature, the latter at high temperature as described above. The nature of  $\text{O}^*$  in the scheme above is not completely clear, except that it is an oxygen atom at the end of an oxygen island and probably next to a metallic Cu atom; this oxygen may well be  $\text{O}^-$  like, and so highly reactive. Some of our high resolution images of these oxygen islands also indicate some morphological differences at the terminal site, with the final atom being relaxed away from other atoms in the chain [20]. The third step in the above scheme simply shows the regeneration of a terminal oxygen atom, by the exposure of what was previously one of the majority adsorbed oxygen species which are not terminal ( $\text{O}_a$ ), which occurs as water is lost. The importance of terminal oxygen atoms in such structures has also been noted recently by Roberts et al. for ammonia reaction with preadsorbed oxygen on Cu(110) [26,27], and by Ruan et al. for the same reactants on Ni(110) [28] and by Crew and Madix for CO oxidation on Cu(110) [29].

The reason that formic acid has a higher reaction probability at room temperature compared with methanol is probably related to precursor state mobility, but may additionally be due to the higher acidity of the acid. The higher molecular complexity of the acid gives it a bigger physisorption heat than the alcohol, which in turn gives it a longer residence time on the surface, and therefore a higher “diffusion circle” [16]. This enables it to find the limited number of active sites with higher probability. However, secondly, the higher acidity of HCOOH may

also give it higher reactivity upon encountering the active site.

## 5. Conclusions

The reaction of formic acid with Cu(110) proceeds as follows. The molecule adsorbs into a weakly held precursor state which has high mobility on the surface, as evidenced by the fact that the sticking coefficient increases from  $\sim 0.1$  on the clean surface to 0.8 for that with preadsorbed oxygen, even when the active sites for adsorption and reaction (oxygen adatoms) are at very low coverage. The molecule reacts much more efficiently with an oxygen saturated surface than does methanol, probably due to its higher heat of physisorption and therefore longer lifetime and extent of diffusion. There is a change in reaction stoichiometry, independent of oxygen coverage, with two molecules of formic acid reacting with each adsorbed oxygen atom below  $\sim 450$  K, but only one reacts at higher temperatures. This relates to the stability of the formate intermediate; the rate of dehydrogenation of this species becomes fast at temperatures above its desorption peak temperature, such that both hydrogens from one molecule react with an oxygen atom to produce water. Because there are so few active sites present with 0.5 monolayers of oxygen predosed the reaction rate begins low at high surface temperatures and increases as oxygen is removed from the surface. There is a temperature range of unusual behaviour between 340 and 430 K, where the reaction probability decreases after an initial short period of high sticking, with little total formic acid uptake. This is due to compression of the oxygen adlayer into a  $c(6 \times 2)$  structure, which is unreactive, and the formation of phase separated  $p(4 \times 1)$  and  $p(3 \times 1)$  regions in which the formate resides. At temperatures lower than this the reactivity is higher, apparently because less of the oxygen is compressed into the  $c(6 \times 2)$ , and the extent of precursor diffusion is greater. At higher temperatures the reactivity is higher because the formate is unstable and therefore does not block sites or compress the oxygen layer; all the oxygen is removed by reaction under these circumstances. TPD shows that formate adsorbed on the half monolayer

oxygen layer gives a low temperature state. This appears to be associated with Cu(II) oxide on the surface by comparison with desorption from Cu(I) and (II) oxide powders, and therefore we infer that the  $c(6 \times 2)$  structure which coexists with the formate is a surface compound of this form. On the surface with  $1/4$  monolayer of oxygen at 300 K or above, all the oxygen is cleaned off by reaction with the acid to produce formate in a simple  $c(2 \times 2)$  structure.

## References

- [1] D. Ying and R.J. Madix, *J. Catal.* 61 (1980) 48.
- [2] I. Wachs and R.J. Madix, *Surf. Sci.* 84 (1979) 375.
- [3] M. Bowker and R.J. Madix, *Surf. Sci.* 102 (1981) 542.
- [4] D. Outka, R.J. Madix and J. Stohr, 164 (1985) 235.
- [5] B. Sexton, *Surf. Sci.* 88 (1979) 319
- [6] B. Hayden, K. Prince, D. Woodruff and A. Bradshaw, *Surf. Sci.* 133 (1983) 589.
- [7] M. Crapper, C. Riley, D. Woodruff, A. Puschmann and J. Haase, *Surf. Sci.* 171 (1986) 1.
- [8] M. Bowker, H. Houghton and K.C. Waugh, *J. Chem. Soc. Faraday I* 77 (1981) 3023.
- [9] M. Bowker, R. Hadden, H. Houghton, J. Hyland and K.C. Waugh, *J. Catal.* 109 (1988) 263.
- [10] K.C. Waugh, *Catal. Today* 15 (1992) 51.
- [11] P. Taylor, P. Rasmussen, C. Ovesen, P. Stoltze and I. Chorkendorff, *Surf. Sci.* 261 (1992) 191.
- [12] M. Bowker, P. Pudney and C. Barnes, *J. Vac. Sci. Technol. A* 8 (1990) 816.
- [13] P. Pudney and M. Bowker, *Chem. Phys. Lett.* 171 (1990) 373.
- [14] P. Kisliuk, *J. Phys. Chem. Solids* 3 (1957) 95.
- [15] D.A. King and M. Wells, *Proc. R. Soc. London A* 339 (1974) 245.
- [16] M. Bowker, *Surf. Rev. Lett.* 1 (1994) 549.
- [17] F. Henn, J. Rodriguez and C. Campbell, *Surf. Sci.* 236 (1990) 282.
- [18] S. Francis, F.M. Leibsle, S. Haq, N. Xiang and M. Bowker, *Surf. Sci.* 315 (1994) 284.
- [19] F.M. Leibsle, S. Francis, S. Haq N. Xiang and M. Bowker, *Phys. Rev. Lett.* 72 (1994) 2569.
- [20] F.M. Leibsle, S. Haq and M. Bowker, in preparation.
- [21] M. Bowker and E. Rowbotham, in preparation.
- [22] D. Coulman, J. Winterlin, J. Barth, G. Ertl and R. Behm, *Surf. Sci.* 240 (1990) 151.
- [23] J. Mundenar, A. Baddorf, E. Plummer, L. Sneddon, R. DiDio and D. Zehner, *Surf. Sci.* 188 (1987) 15.
- [24] B. Hillert, L. Becker, M. Pedio and J. Haase, *Europhys. Lett.* 12 (1990) 247.
- [25] R. Feidenhans'l, F. Grey, M. Nielsen, F. Besenbacher, F. Jensen, E. Laegsgaard, I. Stensgaard, K. Jacobsen, J. Norskov and R. Johnson, *Phys. Rev. Lett.* 65 (1990) 2027.
- [26] B. Afsin, P. Davies, A. Pashusky, M. Robert. and D. Vincent, *Surf. Sci.* 284 (1993) 109.
- [27] A. Carley, P. Davies, M. Roberts and D. Vincent, *Topics Catal.* 1 (1994) 35.
- [28] L. Ruan, I. Stensgaard, E. Laegsgaard and F. Besenbacher, *Surf. Sci.* 314 (1994) L873.
- [29] W. Crew and R.J. Madix, *Surf. Sci.* 319 (1994) L34.